STRUCTURE-BASED VIRTUAL SCREENING AND MOLECULAR DYNAMICS APPROACHES TO TARGET CYP9E2 FOR COMBATING INSECTICIDE RESISTANCE

K. Begum[1,Þ], M. Haseeb[2, Þ,*], R. Bano[3] and S. Khanam[1,*]

[1]Department of Zoology, Women University, Swabi Main Campus Kotha, Khyber Pakhtunkhwa, Pakistan
[2]Department of Molecular Science and Technology, Ajou University Suwon 16499, Korea
[3]Department of Allied Health Sciences, City University of Science and Information Technology, Peshawar. Pakistan
[*]Corresponding Author E-mail: haseeb@ajou.ac.kr ;
[Þ] These authors contributed equally to this work.

ABSTRACT

Insecticide resistance in pests such as bed bugs, mosquitoes, and cockroaches poses a major challenge in urban pest management and public health by reducing the effectiveness of insecticides and increasing control costs. One of the primary mechanisms underlying insecticide resistance is cytochrome P450-mediated metabolic detoxification. The present study focuses on targeting CYP9E2, a member of the Cytochrome P450 monooxygenase enzymes involved in xenobiotic metabolism and detoxification, to identify potential inhibitors that could overcome insecticide resistance. Structure-based virtual screening, molecular docking, and molecular dynamics simulations were employed to identify potent CYP9E2 inhibitors. A three-dimensional model of CYP9E2 was constructed, and the binding interactions between the selected compounds and key active-site residues were comprehensively analysed. Additionally, the ADMET and agrochemical-likeness (ag-like) properties of the shortlisted inhibitors were evaluated to assess their potential as agrochemical agents. The results indicate that two compounds, ZINC09060935(ethyl3-{[(2-hydroxyethyl)(methyl)carbamoyl]amino}-7,7-dimethyl-7,8-dihydro-5H-pyrano[4,3-b]thieno[3,2-e]pyridine-2-carboxylateand) and ZINC32091018 (1-(3-Chlorophenyl)-6,7-dimethoxy-1,4-dihydroindeno[1,2-c]pyrazol-3-yl)(morpholino) methanone), are promising candidates with potential inhibitory activity against CYP9E2. The ADMET and ag-like predictions confirmed agrochemical-likeness criteria of the lead compounds, indicating their potential as CYP9E2 inhibitors. However, further in vitro and in vivo experiments can validate the effectiveness, safety, and applicability of these newly developed resistance-modulating agents for pest management.

Keywords: small-molecule inhibitor, MD simulation, insecticide resistance, CYP9E2, cytochrome P450.

Received January 16, 2026 Published Online October 19, 2026 https://doi.org/10.36899/JAPS.2027.1.0002

INTRODUCTION

Bed bugs, mosquitoes, and cockroaches are among the insects that cause major issues in human habitations. These insects can cause irritation, impair quality of life, and even contribute to the mechanical spread of infections (Brenner and Kramer, 2019; WHO, 2020). The family Cimicidae encompasses bed bugs, which are obligate blood-sucking ectoparasites of humans and have been one of the most prevalent and irritating pests throughout human history (Akhoundi et al., 2020; Cooper and Harlan, 2011). *Cimex lectularius* (Hemiptera; Cimicidae, Carl Linnaeus, 1758) and *Cimex hemipterus* (Fabricius, 1803), the two widespread species, feed entirely on humans and are responsible for significant infestations worldwide (Akhoundi et al., 2020). The number of bed bug infestations has increased globally (Alizadeh et al., 2018). Bed bug bites can cause allergic skin reactions, including red rash or sometimes severe itching, which can lead to infection or even no reaction based on the immunological response of an individual and history of exposure (Miller and Rogers, 2012).

Similarly, mosquito-borne diseases spread by *Aedes aegypti* (Diptera: Culicidae) (Linnaeus, 1762), including dengue, Zika, and chikungunya, continue to pose a major global public health challenge. Among these, dengue is the most widespread, causing millions of infections each year and resulting in substantial morbidity and mortality worldwide (WHO, 2002; Strode et al., 2008; Ishak et al., 2017). Likewise, cockroaches, common pests in human dwellings, transfer pathogens and contribute to health issues such as asthma, allergies, and psychological stress (Gore and Schal, 2007; Zhou et al., 2014; Gondhalekar, 2019).

Globally, the development of pesticide resistance has been one of the major reasons for the resurgence of insects (Myamba et al., 2002; Romero et al., 2007; Doggett et al., 2012). Insecticide resistance in *C. lectularius* and *C. hemipterus* has been well documented worldwide, particularly pyrethroid and dichlorodiphenyltrichloroethane (DDT)

resistance (Dang et al., 2017). During the modern resurgence, resistance to carbamates, neonicotinoids, organophosphates, and phenyl pyrazoles has been reported in bed bugs (Romero and Anderson, 2016; Gonzalez-Morales et al., 2021; Soh and Veera Singham, 2021). The development of insecticide resistance in bed bugs is caused by three main resistance mechanisms: insensitivity to the target site, increased metabolic detoxification, and penetration resistance (Davies et al., 2012; Mamidala et al., 2012).

Cytochrome P450 enzymes are a diverse superfamily that catalyse a range of reactions, including oxidation and hydrolysis, and play a key role in Phase I metabolic pathways. These enzymes are essential for the metabolism of both endogenous and exogenous compounds, contributing to detoxification processes by converting insecticides into more excretable and less harmful forms (Mamidala et al., 2012). Bed bugs (*C. lectularius*) have revealed a significant role of cytochrome P450s in insecticide resistance, with high expression levels of multiple cytochrome P450 genes observed in resistant strains, particularly in the cuticle, midgut, and Malpighian tubules (Adelman et al., 2011). Molecular docking research suggests that P450 enzymes can provide cross-resistance to a range of insecticides, including neonicotinoids, organochlorines, and pyrethroids (Dang et al., 2017).

Cytochrome P450s, especially the CYP4, CYP6, and CYP9 families, are well studied for their roles in xenobiotic metabolism and insecticide resistance. These families show broad substrate specificity and high catalytic versatility, making them crucial in mediating resistance across various insecticide classes. In mosquitoes such as *A. aegypti* and *Anopheles gambiae*, Giles, 1902 (Diptera: Culicidae), as well as in the German cockroach *Blattella germanica* (Blattodea: Ectobiidae) (Linnaeus, 1767) and the bed bug *C. lectularius*, overexpression of P450 genes, particularly those belonging to the CYP6 and CYP9 families, has been associated with resistance to insecticides (Feyereisen, 2005; Smith et al., 2019). This genetic diversity and overexpression of P450s, especially in strains like the Richmond strain of bed bugs, highlight the critical role of these enzymes in insecticide resistance (Zhu et al., 2013).

To develop more efficient and targeted insecticides, researchers are focusing on understanding insecticide resistance mechanisms in pests. Innovative insecticides targeting specific cells could help address the challenge of Insecticide discovery; using conventional approaches is prolonged and costly. However, *in silico* tools such as protein-ligand docking, molecular modelling, pharmacophore generation, quantitative structure-activity relationships, and virtual screening have emerged as effective alternatives to speed up the identification of potential drug candidates (Saini and Kumar, 2014).

Considering the crucial role of cytochrome P450 enzymes in insecticide resistance, the current study was designed to identify new CYP9E2 inhibitors using structure-based virtual screening, molecular docking, and molecular dynamics simulations. Two promising inhibitors, ZINC09060935 and ZINC32091018, showed strong binding interactions with key enzyme residues, indicating their potential in combating insecticide resistance. Collectively, these findings suggest that further in vitro and in vivo validation can confirm the efficacy of potential candidates for combating insecticide resistance.

MATERIALS AND METHODS

Library preparation: The reported inhibitors for Cytochrome P450 in insects were retrieved from available literature. Initially, five reference ligands reported as Cytochrome P450 inhibitors were selected based on their experimentally reported inhibitory potential and relevance to insecticide resistance mechanisms. The ligand structures were taken from PubChem and downloaded in SDF format (https://pubchem.ncbi.nlm.nih.gov/). A multifunctional chemical library of around 19 million compounds was downloaded from the ZINC database (Table 1) (Irwin et al., 2020). Then, the MOE (version 2022.02) software's "sdwash" tool was utilized to further refine these structures. Explicit hydrogen atoms were added along with the protonation of strong bases and deprotonation of strong acids at PH 7.0. A maximum of ten tautomeric states was specified for every ligand, and intramolecular bond lengths were optimized to ideal levels (Clark et al., 2006). Disconnected salts were removed along with water and other residues, and the largest fragments were kept in the library. The MMFF94x force field was then used to calculate the partial charges of the ligands. Subsequently, energy of the chemical library was minimized using the MMFF94x force field till a root-mean-square gradient of 0.1 was attained.

Molecular fingerprint and similarity search: A distinct molecular fingerprint was assigned to each ligand in the screening library using the bit-packed MACCS structural keys (FP: BIT_MACCS) system. An internal script written in MOE Support Vector Language was used to identify chemical structures and showed at least 70–80% similarity to the reference inhibitors of Cytochrome P450. Reference molecules with drug-like physiochemical properties were isolated as Cytochrome P450 inhibitors using the fingerprint-based similarity metric, the Tanimoto coefficient (TC). The Tanimoto coefficient was computed as #AB/ (#A + #B − #AB), where “A” and “B” represent the two fingerprints and “#” indicates the number of features in each fingerprint. Structures similar to the known ligands were considered more likely to yield

hits in a virtual screen. The resulting set of 2066 ligands was subjected to structure-based virtual screening and molecular docking.

Homology modeling and protein structure preparation: The amino acid sequence of CYP9E2 was retrieved using a search on UniProt (UniProt, 2025). The sequence was saved in FASTA format for subsequent analysis. The workflow of the study is illustrated in Fig.1. To predict the 3D structure of the protein, homology modeling was performed. The Protein Data Bank (PDB) was searched to find suitable templates. The retrieved amino acid sequence was then submitted to the Swiss-Model database (Waterhouse et al., 2018) and I-TASSER (Zhou et al., 2022) to generate more accurate 3D models. However, the final model selected for further analyses was the I-TASSER model due to structural quality parameters, including Z-score and C-score values.

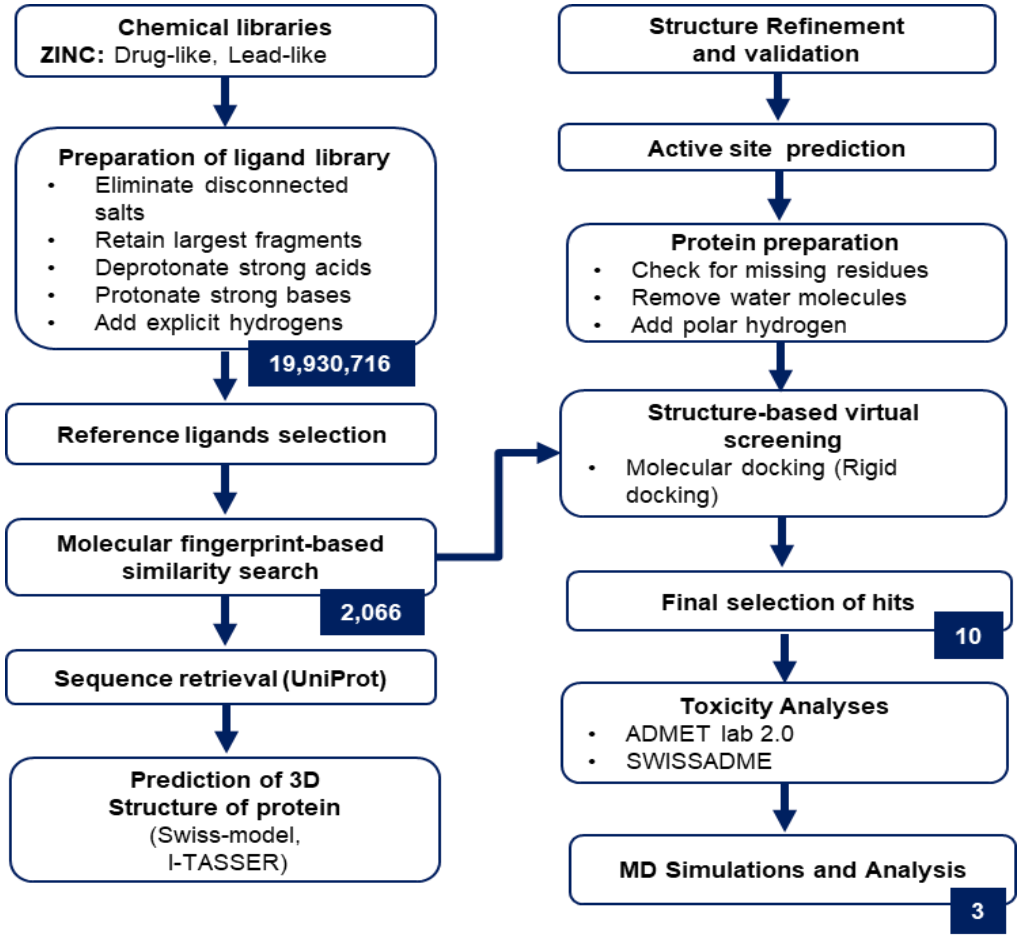

Fig. 1. The overall summary of the virtual screening workflow for the identification of lead compounds. The dark-blue boxes indicate the number of ligands carried forward into the next level.

Following prediction of the 3D structure, the model was protonated at pH 7.0. Energy minimization was then performed in MOE (version 2022.02) using the Amber12: EHT force field, continuing until the root-mean-square gradient reached 0.01. The predicted model was further refined and evaluated using GalaxyWEB (Ko et al., 2012), 3D Refine (Bhattacharya et al., 2016), Verify3D, Pdbsum, and ERRAT. The model's refinement score was good. The selected model consists of 28 helices, 3 Beta turns, and 4 sheets (Fig. 2A, D). To improve the quality assurance of the predicted structure, it was further validated using ProSA-WEB (Wiederstein and Sippl, 2007) and RAMPAGE (Lovell et al., 2003). The structure of the selected protein revealed 90.658% residues in the favoured and allowed regions, 5.520% residues in the permitted region, and 3.822% in the exception area after examining the Ramachandran plot (Fig. 2C, D). These structural parameters of the protein indicated that it was of high quality, adequate and stable.

Active site prediction: The active site was predicted using the Site Finder module in MOE (version 2022.02) and the online servers 3DLigandSite (Wass et al., 2010), COACH (Yang et al., 2013), and CASTp version 3.0 (Tian et al., 2018).

Molecular docking: The docking process was carried out using MOE (2022.02), employing the standard ligand placement method. The triangular matcher algorithm was applied to determine the most suitable poses for the docked molecules. The simulated poses were rescored using the London dG scoring function. London dG generated the best ten ranked poses for each molecule, which were further minimized utilizing the Force field refinement algorithm. All compounds were ranked as per their S-score, binding affinity and Root-Mean-Square Deviation (RMSD) values. The aim was to select only the top pose compounds that actively bind to the target protein with a good docking score. BIOVIA-Discovery Studio visualizer (v21.1.0.20298) was used for the prediction of binding interactions and hydrogen bonding between ligands and the target protein (2021). Initially, **t**he top 10 compounds with a binding score of -9.582 kcal/mol and greater than -9.582 kcal/mol were selected using MOE (2022.02). Subsequently, the top two compounds with docking scores greater than -9.770 kcal/mol were selected for further detailed molecular dynamics (MD) simulations.

Molecular dynamics simulations: MD simulations of the top two hits and permethrin as an insecticide bound to CYP9E2 have been performed using the CHARMM36 force field (Lee et al., 2016) in GROMACS v2022.4 (2022a). Docked complexes solvated within the dodecahedron boxes lined with the rigid water model, TIP3P. CGENFF server was used for retrieving the ligand topology (https://cgenff.umaryland.edu/). A proper proportion of counter ions (Na^+/Cl^-) was added to neutralize the system. The steepest descent algorithm was used to minimize the system's energy to 0.001 kJ/mol/nm. The system was then adjusted for temperature and pressure up to 100 ps, using the Parrinello-Rahman (Parrinello and Rahman, 1981) and Nose-Hoover methods. To prevent structural distortions, position constraints were imposed on the skeleton of heavy atoms during the equilibration process. Long-range electrostatic interactions were treated with cubic interpolation using the particle mesh Ewald algorithm (Darden et al., 1993), while short-range Van der Waals and Coulomb interactions were treated with a 12 Å cutoff.

The docked complexes were considered for a 100 ns MD simulation study using constant pressure and constant temperature (NPT ensemble). All bonds, including hydrogen atoms, were constrained using an algorithm, the Library of Integrated Network-Based Cellular Signatures (LINCS) (Hess et al., 1997) and then 2-ps was used for saving structural coordinates. Xmgrace (Turner, 2009), MOE 2022.02, and the BIOVIA-Discovery Studio visualizer (v24.1.0.23298) was used to create the plots and structure visualizations (2021). After the MD simulation was successfully completed, several parameters were evaluated, including the Radius of gyration (Rg), root-mean-square deviation (RMSD), root-mean-square fluctuation (RMSF), the number of hydrogen bonds, and the distance between the protein and ligands.

Toxicity Analyses: SWISSADME (Daina et al., 2017) and ADMETlab 2.0 (Xiong et al., 2021) were used for physicochemical and ADMET (Absorption, distribution, metabolism, excretion and toxicity) properties of the top ten compounds. Tice's rule of similarity with agrochemicals was applied to assess agrochemical-likeness (ag-like) of the compounds, which specify a molecular weight between 150 and 500 Da, polar surface area $\leq 142 Å^2$, a Log P ranging from 0 to 5, a maximum of 12 rotatable bonds, number of hydrogen bond donors ≤ 2 and 1 to 8 hydrogen bond acceptors (Rosado et al., 2019, Tice, 2001).

RESULTS

Potential inhibitors of cytochrome P450 enzymes responsible for insecticide resistance were identified using computer-aided drug design (CADD), and a novel binding site was proposed, along with efficient chemicals that can be used for the control of insects. An extensive review of the literature shows that cytochrome P450 monooxygenases perform a crucial role in insecticide detoxification. Specifically, the CYP9 subfamily has been known as a primary mediator of metabolic resistance in several key insect species, such as *A. aegypti*, *C. lectularius* and *B. germanica*.

CYP9E2 from *Blattella germanica* contained 533 amino acids. The sequence was retrieved from UniProt in FASTA format, and a homology model of the protein was built. The model built by the Swiss Model database showed 41.27% sequence identity (PDB ID: 8SO1). The sequence similarity of I-TASSER (Suite v5.1) was good compared to the Swiss model, as the normalization Z-score was 4.05 (PDB ID: 1TQN).

Thus, the protein model of CYP9E2 was selected from I-TASSER (Suite v5.1) based on the z-score, sequence identity and alignment scores, as structure prediction requires closely related templates from the PDB; therefore, that model was downloaded for further docking and virtual screening.

I-TASSER accurately generates up to 5 predicted models for each sequence, ranked by C-score, and the normal range for a C-score ranges from -5 to 2. The best model was selected based on the highest confidence score (C-score -0.09), which was further evaluated and refined.

Prediction of active sites: The active site residues of CYP9E2 were identified using MOE (SiteFinder), the CASTp server, 3DLigand, and the COACH server, including polar and charged amino acids such as His, Asp, Ser, and Cys involved in ligand binding and catalytic activity. A consensus analysis of the results from these tools revealed the active site (highlighted in red) and identified key amino acids critical for docking (Fig. 2B). The predicted active sites of CYP9E2 comprised of the following residues: His108, Pro111, Ala116, Phe120, Leu124, Phe125, Asn126, Leu139, Phe143, Gln239, Phe259, Met289, Gln327, Leu330, Phe331, Phe333, Ala334, Thr338, Pro399, Ala400, Phe402, Thr403, Asp404, Ile431, Pro467, Phe468, Gly469, Cys475, Ile476, Gly477, Asn478, Phe515.

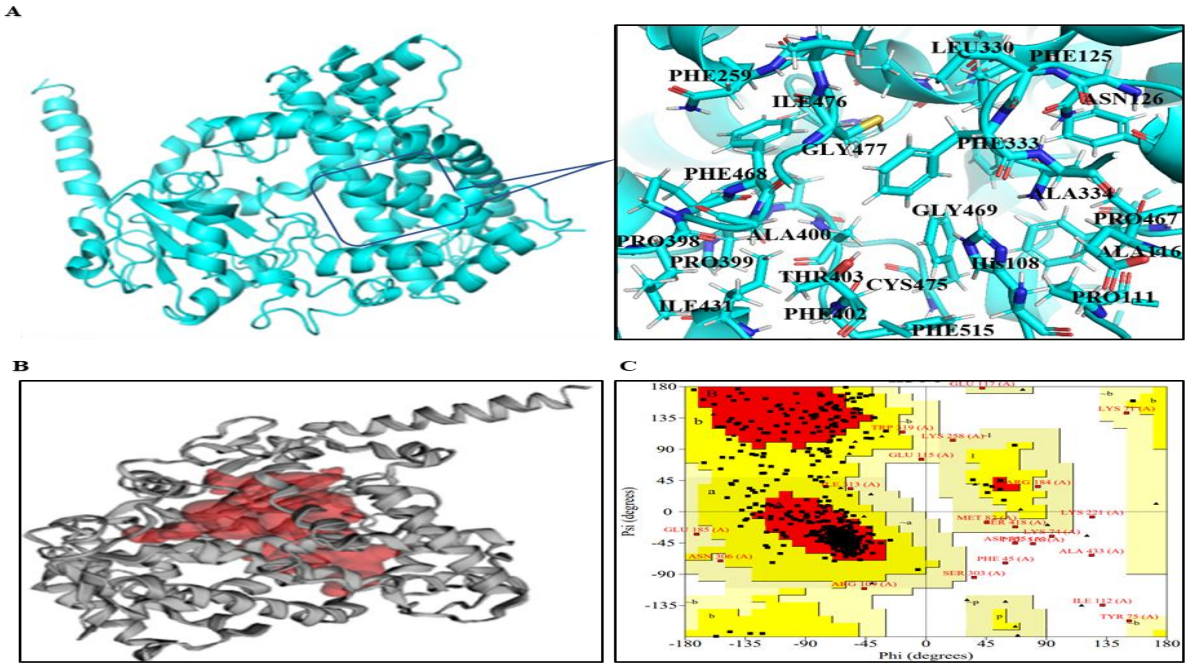

D Structure refinement score of selected 3D model of CYP9e2

Structure Refinement Analysis	Score	%
Residues in most favoured regions [A,B,L]	357	75.8
Residues in additional allowed regions [a,b,l,p]	93	19.7
Residues in generously allowed regions [~a,~b,~l,~p]	13	2.8
Residues in disallowed regions	8	1.7
Number of non-glycine and non-proline residues	471	100
Number of end-residues (excl. Gly and Pro)	2	-
Number of glycine residues (shown as triangles)	32	-
Number of proline residues	28	-
Total number of residues	533	-
Verify3D	86.30	-
*PDBsum	95.5	-
ERRAT	84	-
GalaxyWEB	93.2	-
*Score is the sum of amino acids in allowed and favored region.		

Fig. 2. Prediction and evaluation of the Homology model. (A) Predicted structure and pocket residues representation of CYP9E2. **(B)** Representation of CYP9E2 active site (red color) using MOE, and CastP server. **(C)** RAMPAGE analysis of the target protein. **(D)** Structure refinement score of the selected 3D model of CYP9E2.

Molecular docking: To identify specific and novel ligands for CYP9E2, the target protein was docked against commercially available chemical compounds (Table 1) and reference ligands, known as inhibitors of cytochrome P450 (Table 2). The docked compounds were assessed and ranked based on their docking scores (S scores), RMSD values, binding energies, and interactions with the active site residues.

Table 1. Chemical compound libraries used for ligand screening.

Compound library	Number of compounds
ZINC druglike	14,480,911
ZINC leadlike	5,449,805
Total	**19,930,716**

All ligand libraries were freely obtained from the ZINC database (https://zinc.docking.org/).

Table 2. List of ligands selected as Cytochrome P450 inhibitors

Ligands	2D structures	Target	IC_{50} values	Reference
Ritonavir	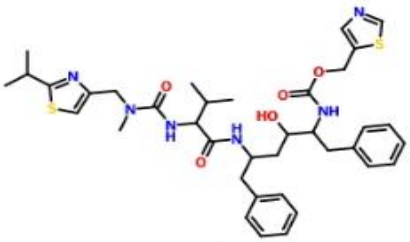	CYP3A	70-130 nM	(Loos et al., 2023)
Permethrin	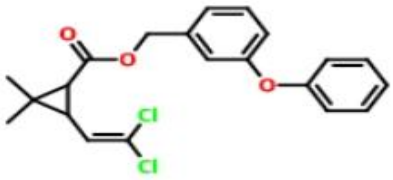	CYP6P4	0.97 µM	(Ibrahim et al., 2016)
Clarithromycin	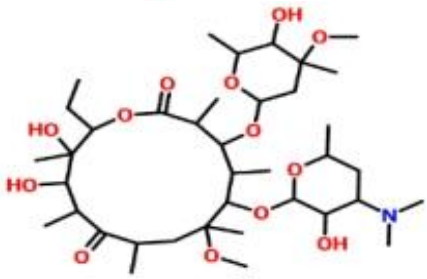	CYP3A4	56 µM	(Zhao et al., 1999)
Diltiazem	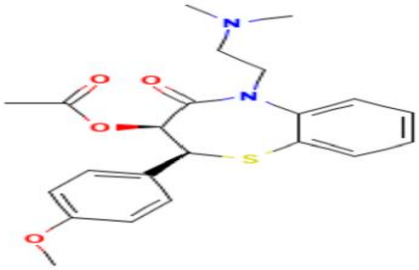	CYP3A4	120 µM	(Sutton et al., 1997)
Itraconazole	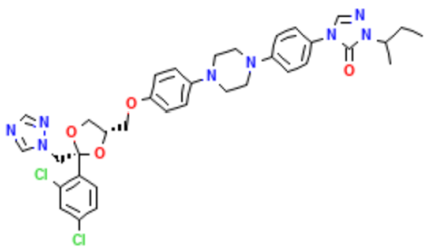	CYP3A4	6.1 nM	(Isoherranen et al., 2004)

IC_{50}: Half maximal inhibitory concentration; µM: Micromolar; nM: Nanomolar

The top ten compounds with the highest scores were further analyzed for their binding interactions, docking scores, and ADMET properties (Table 4 and Table 5).

Table 4. Top 10 compounds selected for CYP9E2 inhibition after virtual screening

ZINC IDs	Binding score (Kcal/mol)	Binding energy	RMSD
ZINC09060935	-10.125	-107.457	1.072
ZINC32091018	-9.966	-56.210	1.342
ZINC06404931	-9.770	-101.525	1.591
ZINC78287601	-9.742	-85.719	0.918
ZINC12750810	-9.737	-75.952	1.878
ZINC89961216	-9.736	-73.169	1.575
ZINC00108562	-9.665	-85.806	0.724
ZINC69828911	-9.611	-91.032	1.373
ZINC78115327	-9.593	-84.945	0.979
ZINC89961217	-9.582	-83.066	1.549

RMSD: Root Mean Square Deviation

Binding Score: Empirically determined fitness approximated from static molecular docking

Binding Energy: Actual thermodynamic affinity (\Delta G) determined from MD simulation trajectories

Table 5. Physiochemical properties of the top 10 compounds

ZINC IDs	MW (g/mol)	NHA	NHD	LogP	LogD 7.4	LogS (ESOL)	BBB	ABS	P-gp	Acute rat toxicity	TPSA	Lipinski Rule	AMES Toxicity	CYP3A4 Inhibitor
ZINC09060935	407.4	6	2	2.8	2.2	-3.4	No	High	Yes	0.07	129.2	Accepted	0.4	Yes
ZINC32091018	439.8	5	0	3.6	2.7	-4.8	Yes	High	Yes	0.4	65.8	Accepted	0.4	Yes
ZINC06404931	371.4	4	0	3.2	3.2	-4.5	No	High	No	0.2	81.1	Accepted	0.4	Yes
ZINC78287601	342.4	4	2	3.4	1.6	-1.8	No	High	Yes	0.2	111.8	Accepted	0.6	No
ZINC12750810	373.4	4	0	3.5	3.1	-4.6	Yes	High	No	0.2	73.3	Accepted	0.4	No
ZINC89961216	361.4	5	2	3.3	1.3	-2.7	No	High	Yes	0.3	102.9	Accepted	0.8	No
ZINC00108562	306.7	3	0	3.2	3.4	-4.0	Yes	High	No	0.3	43.3	Accepted	0.1	Yes
ZINC69828911	349.4	4	2	2.9	2.1	-2.8	No	High	Yes	0.2	102.9	Accepted	0.4	No
ZINC78115327	368.4	4	2	2.5	2.3	-2.5	No	High	Yes	0.2	111.8	Accepted	0.4	No
ZINC89961217	361.4	5	2	2.7	1.4	-2.7	No	High	Yes	0.1	102.9	Accepted	0.7	No

MW: Molecular weight; NHA: Number of Hydrogen bonds acceptor; NHD: Number of Hydrogen bonds donor; LogP: Partition coefficient; LogD: Distribution coefficient; LogS: Solubility; BBB: Blood-Brain Barrier; ABS: Aboroption ; P-gp: P-Glycoprotein; TPSA: Topological Polar surface area; LogS: optimal: higher than -4 log mol/L, LogS <10 µg/mL: low solubility; LogS 10–60 µg/mL: moderate solubility; LogS >60 µg/mL: high solubility; LogP: optimal: 0< LogP <3, LogP <0: poor lipid bilayer permeability, LogP >3: poor aqueous solubility.

Visualization of the residues within approximately 5 Å of the top hits revealed interactions involving both unique and common amino acids identified in the receptor-binding cavities (Fig. 3, 4). The selected top ligands were deeply embedded within the binding pocket and exhibited the lowest binding energies, ranging from -9.5 to -10 kcal/mol. All top-ranked hits demonstrated favourable binding energies and robust interactions. These interactions included hydrogen bonds, hydrophobic interactions, and π-alkyl, π-π stacking, and π-σ bonding between the CYP9E2 active site residues and the top hits. Notably, residues such as Cys, His, and Pro were involved in strong hydrogen bonding, while Thr contributed to both hydrogen bonding and carbon-hydrogen interactions. Additionally, Asn, Phe, Asp, and Ala were involved in carbon-hydrogen interactions. (Fig. 3). Among these compounds, the top two were selected based on their strong binding affinities and favourable interactions with the target protein (Fig. 4).

The docking results confirmed that the compound ZINC09060935 interacts with the key residues of the protein. This compound with a molecular weight of 407.492 g/mol showed the best interaction, lowest (-10.12 Kcal/mol) binding energy and stability inside the druggable pocket of the target protein (Fig. 4A). Thr403 and Phe402 residues established strong hydrogen bonds with bond distances of 2.02Å, 2.25Å, 3.04Å with the carbamate moiety (2-hydroxyethyl) of the ligand (Fig. 4B).

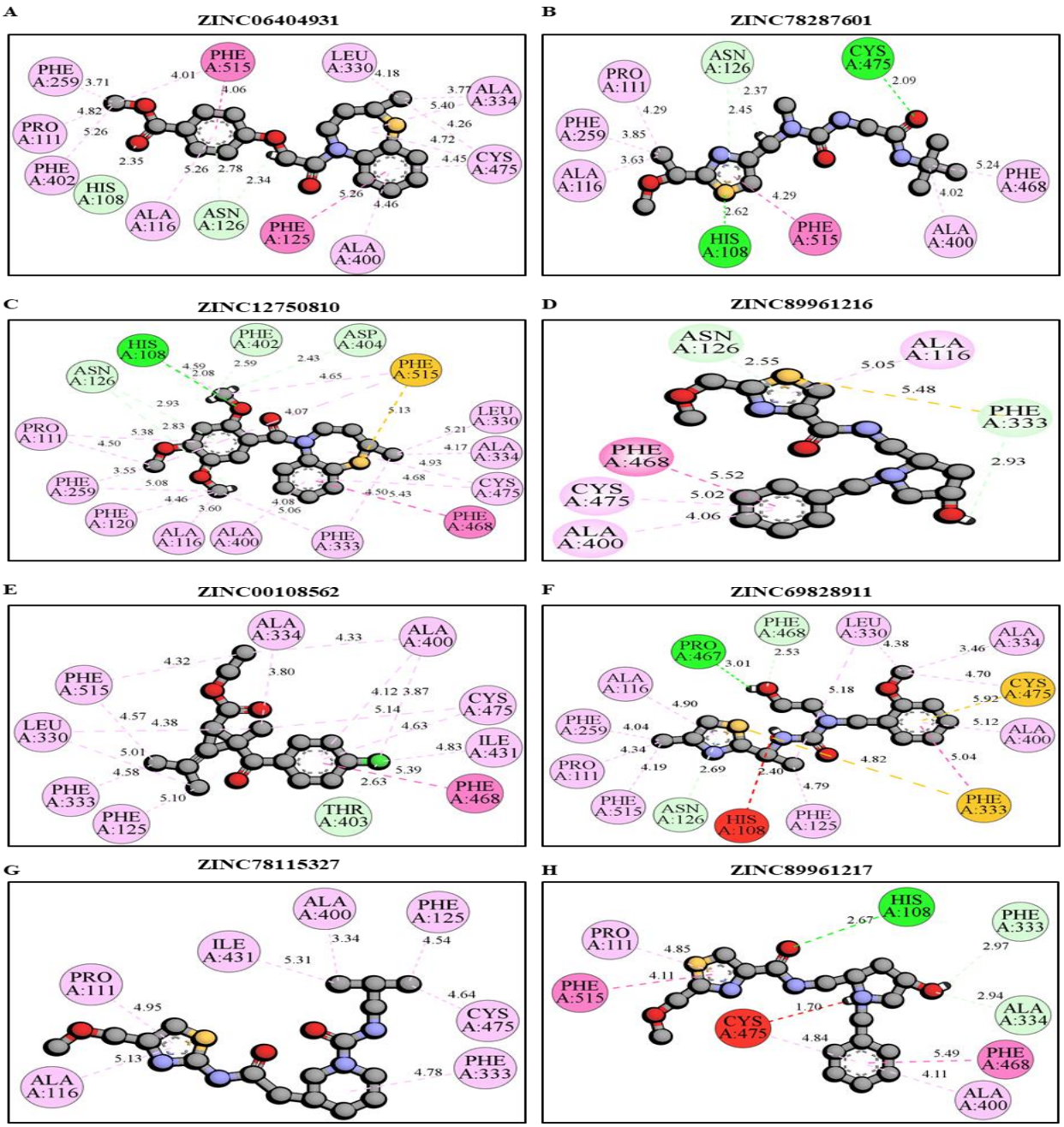

Fig. 3. Distance and interaction analysis of top hits with CYP9e2. (**A-H**) The interaction and distance between top hits and CYP9e2 residues. Dark green residues have a conventional hydrogen bond, whereas light green residues have a carbon-hydrogen bond, pink (Pi-alkyl), dark pink (Pi-pi stacked), purple (Pi-sigma), red (unfavorable donor-donor), and orange (Pi-anion) bonds.

ZINC32091018 showed better binding orientation at the active site cavity of the CYP9E2 protein (Fig. 4C). The compound with a molecular weight of 439.899 g/mol showed a -9.966 Kcal/mol binding score and carbon-hydrogen

bonding with Gly477, Ile476, Leu330, Asn126, and His108. These interactions served to enhance the ligand's stability inside the druggable pocket (Fig. 4C). Dimethoxy-dihydroindeno pyrazol and morphine moieties present in ZINC32091018 were found to form C-H bonding as well as π-stacking and hydrophobic interactions with the key residues shown in Fig. 4D. These findings suggest that these compounds hold significant potential as lead candidates and were further used for MD simulations.

Molecular dynamics simulations: MD simulations were performed to assess critical insights into the structural integrity, stability, and behaviour of the ligand-protein complexes over time. The ligand-protein interactions for the two hits (ZINC09060935 and ZINC32091018), along with the reference insecticide permethrin, were calculated over the simulation time (from the initial conformation at 0 ns and final conformation at 100 ns).

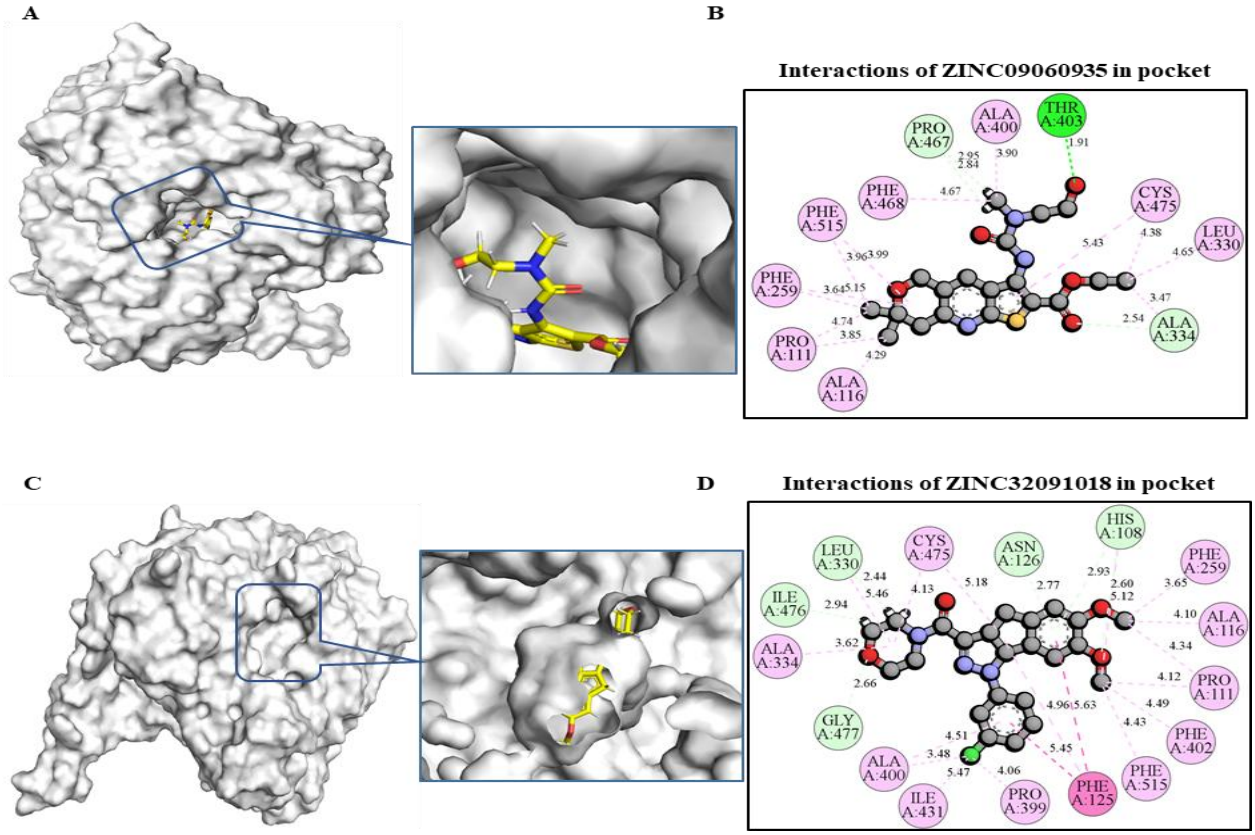

Fig. 4. Interactions of hit compounds with CYP9e2. (A) Surface representation of the receptor and binding pocket of ZINC09060935. **(B)** A detailed interaction of the key residues within 5 Å of ZINC09060935. **(C)** Surface representation of the receptor and binding pocket of ZINC32091018. **(D)** A detailed interaction of the key residues within 5 Å of ZINC32091018.

The initial conformation of permethrin interacted with Phe143, Arg479, Asn478, and Tyr465. These interactions remained stable at 100 ns, except for the Phe143 interaction (Fig. 5A).

For ZINC09060935, the 7,8-dihydro-5H-pyrano[4,3-b]thieno[3,2-e] pyridine scaffold formed π-alkyl interactions with hydrophobic residues Ala116, Pro111, Phe259, and Phe515. Additionally, the methyl 3-{[(propylamino)carbonyl]amino}-2-thiophenecarboxylate moiety interacted with both polar and hydrophobic residues, including Phe468, Pro467, Ala400, Thr403, Cys475, Leu330, and Ala334, through hydrogen bonding and π-alkyl interactions (Fig. 5B). Similarly, for ZINC32091018, the 6,7-dimethoxy-1,4-dihydroindeno[1,2-c]pyrazole scaffold engaged in π-alkyl interactions and hydrogen bonding. Its morpholine ring formed hydrogen bonds with Leu330, Ile476, and Gly477. These findings suggest that Ala334, Leu330, Cys475, Ala400, Phe515, Phe259, Pro111, Ala116, and Phe402 serve as common binding residues for both ZINC09060935 and ZINC32091018, the remaining interacting residues are distinct to each compound (Fig. 5C). Notably, the interacting residues for both compounds remained consistent between their initial and final conformations, emphasizing the stability of these ligands within the binding pocket.

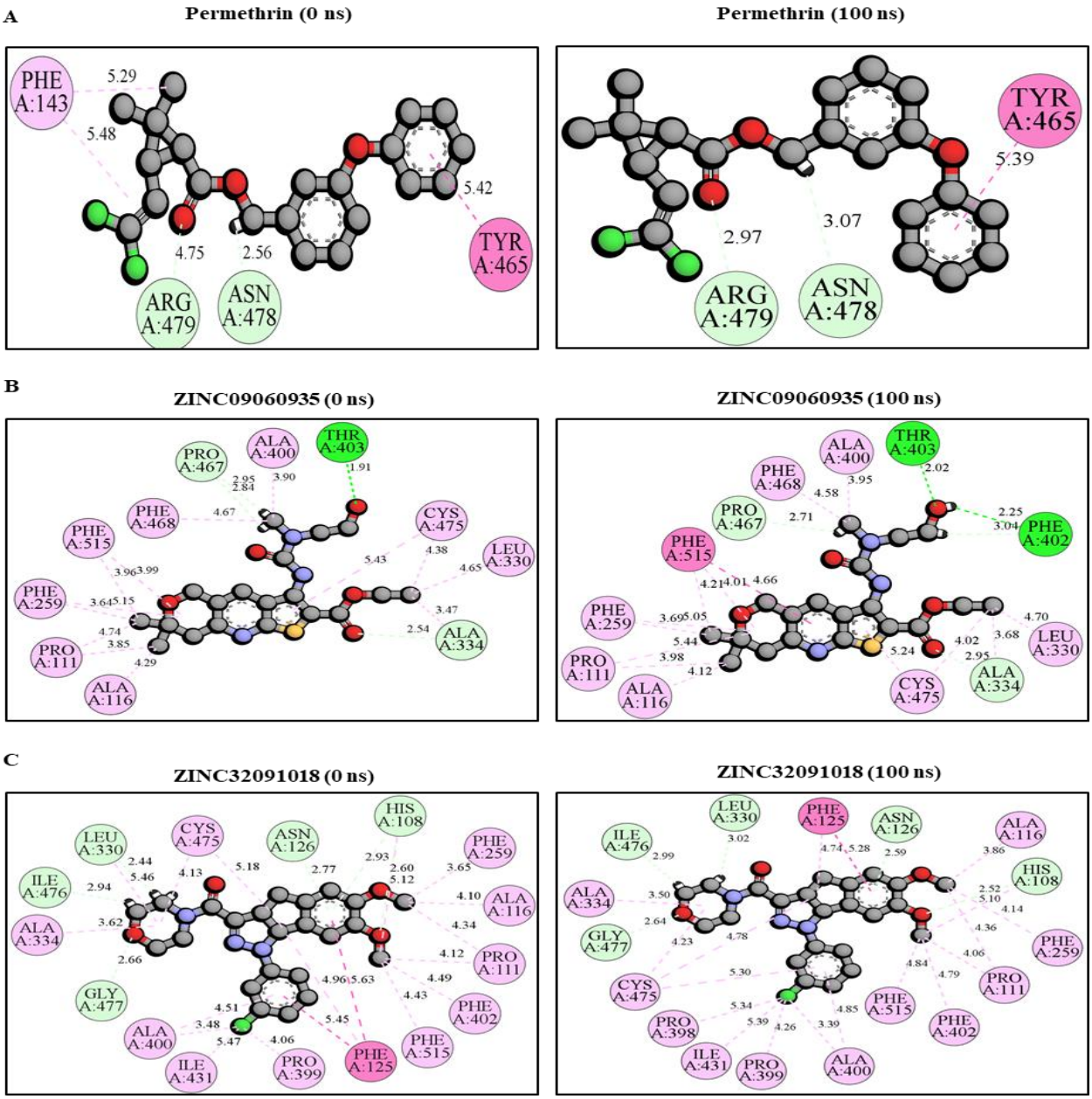

Fig. 5. Time-dependent distance and interaction analysis of CYP9e2 complexes with permethrin, ZINC09060935, and ZINC32091018. (A) The interaction and distance between permethrin and CYP9e2 residues over time, depicted at initial conformation (0 ns), and final 100 ns. **(B-C)** The interaction and distance between the top hits ZINC09060935 and ZINC32091018 over the same time points. Dark green residues have a conventional hydrogen bond, whereas light green residues have a carbon-hydrogen bond, pink (Pi-alkyl), and dark pink (Pi-pi stacked) bonds.

The structural and dynamic stability of the ZINC09060935-CYP9E2, ZINC32091018-CYP9E2, and permethrin-CYP9E2 complexes were evaluated using Rg, RMSD, RMSF, distance, and hydrogen-bond analyses. The simulation results demonstrated that ZINC09060935, ZINC32091018, and permethrin maintained structural stability throughout the 100 ns simulation. The Rg values, averaging 24 Å, indicated consistent compactness and minimal fluctuations across all complexes (Fig. 6A). This stability underscores the strong binding interactions of ZINC09060935 and ZINC32091018 with the CYP9E2 binding site, supporting their potential as effective inhibitors.

The average RMSD values for all three complexes remained around 0.4 Å, confirming the stability of the protein-ligand interactions and the overall integrity of the systems over the simulation period (Fig. 6B). RMSF values for

the complexes were within a range of 0.3-0.5 Å, reflecting minimal fluctuations and a stable binding environment (Fig. 6C).

To gain additional insights, centre-of-mass (COM) distances were monitored over time (Fig. 6D). The top hits, ZINC09060935 and ZINC32091018, consistently maintained a COM distance of ~5 Å, while permethrin exhibited a larger distance of ~15 Å. The greater distance observed in the permethrin complex likely contributed to the reduced interactions compared to the top hits. Hydrogen bond analysis revealed that both ZINC09060935 and ZINC32091018 formed consistent hydrogen bonds with CYP9E2 throughout the simulation, averaging approximately one bond at any given time (Fig. 6E, F). These interactions further confirm the stability and binding efficiency of the top compounds, positioning them as strong candidates for CYP9E2 inhibition.

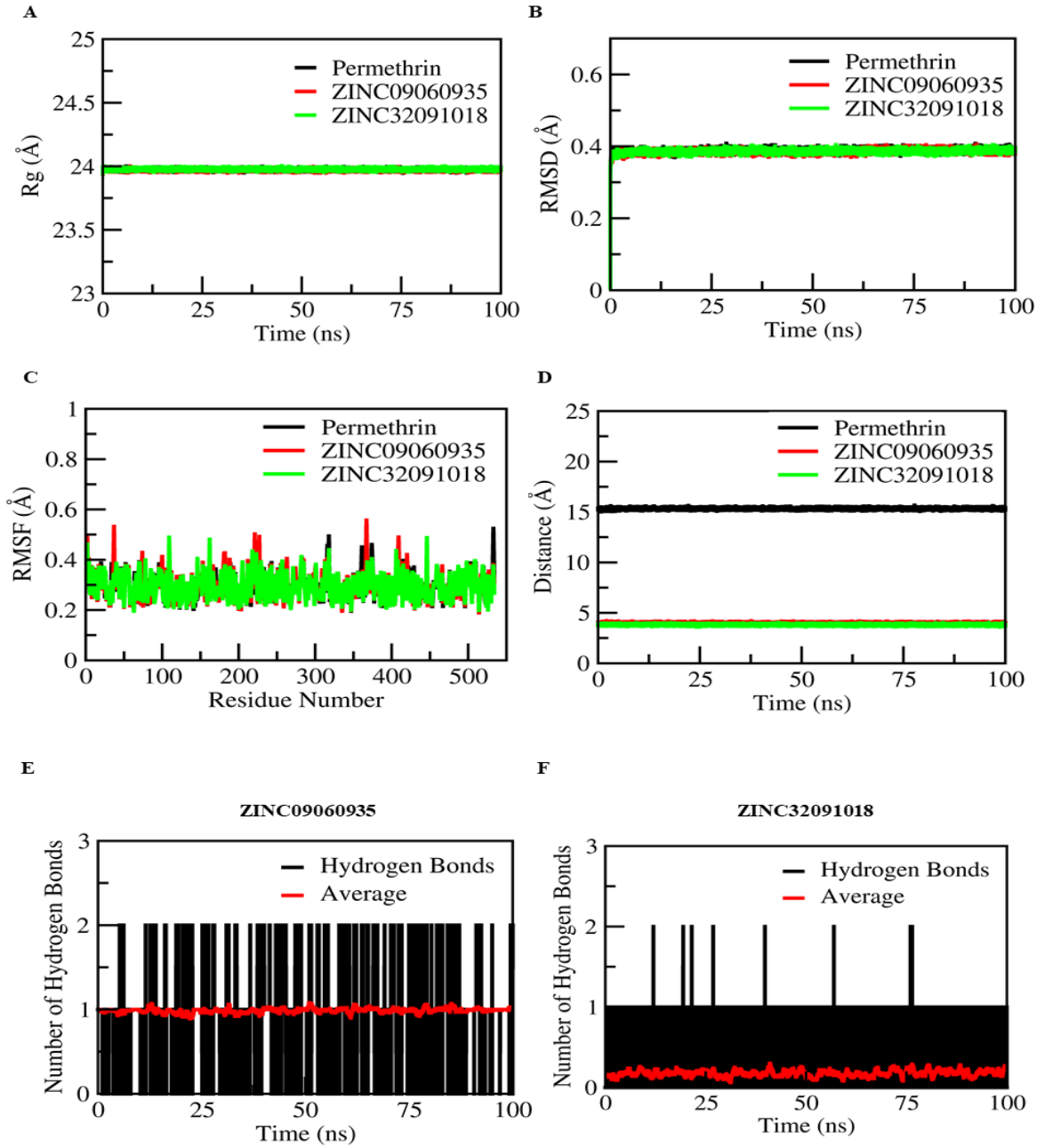

Fig. 6. Trajectory analysis of CYP9e2 complexes with Permethrin, ZINC09060935, and ZINC32091018. (A) The Radius of gyration (Rg). **(B)** The Root-mean-square deviation (RMSD). **(C)** Root-mean-square fluctuation (RMSF). **(D)** The distances between the CYP9e2, permethrin, ZINC09060935, and ZINC32091018. **(E-F)** The number of hydrogen bonds.

The compounds' favorable pharmacokinetic and physicochemical characteristics enhance their potential as promising leads for inhibitor development. The selected compounds exhibited favourable drug-like properties, meeting essential pharmacokinetic and safety criteria. Lipinski's Rule of Five assesses the "drug-likeness" of new molecular entities (NMEs) and predicts their absorption and permeability. According to the rule, drugs with more than 5 hydrogen-bond donors (HBDs), more than 10 hydrogen-bond acceptors (HBAs), molecular weights above 500 g/mol, or a CLogP value exceeding 5 are likely to exhibit poor absorption or permeation. The selected compounds have fewer than 10 rotatable bonds (6 in ZINC09060935 and 4 in ZINC32091018), which enhances molecular stability and bioavailability, as excessive rotatable bonds (>10) are associated with reduced bioavailability.

The topological polar surface area (TPSA), another key indicator of drug-likeness, was well within Veber's rule threshold of 140 Å², with no compound exceeding 129 Å². The selected compounds showed favourable water solubility, partition and distribution coefficients, and other drug-likeness parameters. Additionally, the physicochemical properties of the lead compounds generated by SwissADME and ADMET LAB meet the criteria defined by Tice's Rule, thereby supporting their classification as agrochemical-like (Table 5). The top two hits demonstrated CYP3A4 inhibition and achieved high scores across all evaluated criteria, while complying with Lipinski's Rule of Five and Veber's rule. According to Tice's rule, most insecticides fall within the MLogP range of 1.7–3.5, with an average of 2.6 and ZINC09060935 and ZINC32091018 aligned with this pattern.

DISCUSSION

The excessive use of fumigation and insecticides for pest control has contributed to the emergence of insecticide resistance in various insect species (Amezian et al., 2021). One major factor driving this resistance is the elevated expression of cytochrome P450 enzymes, which plays a pivotal role in detoxifying insecticides. This study aimed to identify potential inhibitors targeting cytochrome P450 enzymes involved in metabolic detoxification in insects, specifically *C. lectularius, A. aegypti,* and *B. germanica*, through computational approaches.

Cytochrome P450 enzymes exhibit species-specific variations (Chan et al., 2014), yet our findings revealed that the CYP9 subfamily is commonly implicated in insecticide resistance in *C. lectularius, A. aegypti and B. germanica*. Targeting this subfamily with effective inhibitors could help to mitigate resistance. As the 3D structure of the target protein was not available in the PDB, it was predicted using I-TASSER and Swiss-Model. A high C-score indicates that the predicted structure is of high quality, and vice versa (Zhang and Skolnick, 2004). The predicted model demonstrated good scores and accuracy, enabling further molecular docking studies conducted using MOE software.

Molecular docking analyses are crucial in drug discovery as they can predict a ligand's preferred orientation with a protein (Ibrahim et al., 2024). Docking results highlighted strong interactions and binding affinities of the selected compounds, with the top ten exhibiting the highest docking scores and binding energies against the target protein. Among these, ZINC09060935 and ZINC32091018 demonstrated the most favourable binding energies. The binding energies and docking scores offer key insights into the stability and binding affinities of the protein-ligand interactions (Alruhaimi et al., 2024). However, while binding energy indicates affinity, it alone cannot guarantee inhibitory activity. The binding conformation and interactions with critical amino acid residues in the active site significantly influence a compound's inhibitory potential (Ononamadu et al., 2021).

The selected top hits exhibited extensive interactions with critical residues of the target protein. For instance, ZINC09060935 formed four hydrogen bonds, with its carbamate moiety establishing three stable conventional hydrogen bonds with Phe402 and Thr403, and additional carbon-hydrogen bonds. These interactions were within the optimal range for hydrogen bonding (2.5–3.5 Å), confirming the accuracy of the molecular docking studies (Hubbard and Haider, 2010). The second compound, ZINC32091018, formed five hydrogen bonds with key residues His108, Asn126, Leu330, Ile476, and Gly477. Both compounds also displayed hydrophobic and π-stacking interactions, indicating that their functional groups effectively interacted with CYP9E2 binding residues.

In contrast, permethrin exhibited fewer interactions. It was selected as a positive control due to its proven insecticidal activity via sodium-channel disruption (Wismer, 2016) and its extensive use against populations of these three pests susceptible to pyrethroids (Du et al., 2016; Feng et al., 2023). Its carboxylic moiety formed only two carbon-hydrogen bonds with Arg479 and Asn478, and its phenoxy benzyl ring formed a π-stacked interaction with Tyr465 but lacked stable hydrogen bonds. These results suggest weaker binding compared to the top hits.

Pyrethroid insecticides, such as permethrin, are widely used to control insect pests due to their strong insecticidal effects and low mammalian toxicity (Du et al., 2016; Feng et al., 2023). Permethrin functions by binding to sodium channels, causing nerve hyperactivity and leading to paralysis and death of insects (Wismer, 2016). During the 100 ns molecular dynamics (MD) simulations, the interactions between ZINC09060935 and ZINC32091018 with the active-site residues of CYP9E2 were analyzed alongside those of permethrin. The top hits demonstrated more robust and

consistent interactions throughout the simulation, supporting their potential as effective inhibitors of CYP9E2 to combat insecticide resistance in *C. lectularius*, *A. aegypti* and *B. germanica*.

Several orthogonal metrics offer the same outcome when the 100 ns MD simulations were used to test whether these favourable docking poses were associated with actual stable complexes compared to static docking. The quality set of descriptors employed in the computational drug-discovery literature to differentiate between transient or non-specific binding and stable protein–ligand complexes is RMSD, RMSF, radius of gyration and hydrogen-bond persistence (Arefin et al., 2021; Ghahremanian et al., 2022).

Fluctuations influence the stability of a protein-ligand complex in a dynamic state in the backbone of individual amino acid residues (Senthil et al., 2019). Quantitative metrics such as RMSD and RMSF are critical indicators of this stability. RMSD measures the deviation of atomic positions from their reference coordinates over time, providing insights into structural variations during MD simulations. For ZINC09060935, ZINC32091018, and the positive control permethrin, the RMSD remained stable with an average value of approximately 0.4 Å over the 100 ns simulation, confirming their stability within the CYP9E2 binding cavity. A docking program is considered reliable when the RMSD is ≤2.0 Å compared to the native binding position of the control ligand (Ramirez and Caballero, 2018). The low RMSD values observed here validate the structural stability of the protein-ligand complexes and confirm the reliability of the docking protocol. The ligand fitness and binding interactions indicate that critical binding interactions crucial to ligand efficacy are effectively captured by the docking protocol.

The RMSF determines a protein's specific amino acid residues (Ibrahim et al., 2025). RMSF analysis was conducted to evaluate residue-specific flexibility in CYP9E2 ligand complexes. RMSF provide insights into the dynamic behavior of the protein–ligand complex and locates specialised protein regions that exhibit considerable conformational changes in response to ligand binding (Hassan et al., 2023). The RMSF value of ZINC32091018 demonstrated superior stability to ZINC09060935 and permethrin, indicative of better potential as a Cyp9E2 inhibitor. The RMSF profiles of ZINC09060935 and permethrin showed very slight fluctuations, indicating more flexible areas of Cyp9E2. However, these complexes maintained stable conformations throughout the simulation.

The radius of gyration (Rg) measures the distribution of a protein's atoms around its axis and reflects structural compactness during simulations. It is essential to determine structural stability and conformational changes during MD simulations (Swati et al. 2024). The Rg values for ZINC09060935, ZINC32091018, and permethrin remained super stable, with a maximum value of ~24 Å, confirming the system's compactness and structural integrity throughout the simulation. These findings are consistent with Bagewadi et al. (2023), who reported that Consistent Rg values indicate stability, while deviations may suggest protein destabilisation.

The centre-of-mass (COM) distances between the ligands and the protein were monitored over time to assess interaction stability. Permethrin showed a higher average centre-of-mass distance between the ligand and the protein complex than ZINC09060935 and ZINC32091018. These two compounds maintained consistent distances of ~5 Å, while permethrin exhibited a distance of ~15 Å. The greater distance for permethrin likely explains its reduced interactions compared to the top hits. The lower average distance indicates a closer proximity and potentially more stable protein-ligand binding (Alshaghdali et al., 2024). Hydrogen bond (H-bond) kinetics were analyzed to assess interaction stability. The stability and specificity of protein-ligand interactions depend significantly on the formation of hydrogen bonds (Rana et al., 2025). The two hits, ZINC09060935 and ZINC32091018, formed more H-bonds than permethrin, indicating their potential as strong inhibitors of CYP9E2.

The significant physicochemical parameters considered for a compound to be drug-like are solubility, polarity, flexibility, saturation, lipophilicity and size. A compound must fall inside the pink area indicated by certain characteristics illustrated on each axis to be classified as "drug-like (Chibuye et al., 2025). Notably, the compounds were positioned within the optimal "pink area" of the bioavailability radar, indicating that their physicochemical attributes align with those of bioavailable drugs. The red-distorted hexagon within the pink shade further confirmed their potential as effective and safe candidates for further development (Saleh et al., 2021).

ZINC09060935 and ZINC32091018 revealed desirable physicochemical properties and were aligned with the ag-like parameters of the Tice Criterion, such as the compounds' LogP values (Rosado et al., 2019).

These compounds' alignment with Tice's Rule parameters, notably their molecular weight and LogP, fall within the range of agrochemicals and supports their potential suitability as agrochemical candidates. The comparison of drug-likeness and agrochemical-likeness of a candidate is important, as agrochemicals usually exhibit lower lipophilicity and smaller size than therapeutic compounds, in compliance with the validation underlying Tice's adaptation of Lipinski's original framework (Souza et al., 2025).

These findings affirm the physicochemical and agrochemical-likeness (ag-likeness) properties of the selected compounds as promising candidates for inhibiting cytochrome P450 and addressing insecticide resistance in insects.

Conclusion: In conclusion, all the selected compounds showed strong protein-binding interactions and high scores. However, ZINC09060935 and ZINC32091018 demonstrated the highest docking scores and strong interactions with the target protein. According to the current study, these compounds could serve as effective inhibitors of cytochrome P450 (CYP9E2) in insects and provide a theoretical basis for developing improved insecticides. As computational predictions alone do not confirm a compound's efficacy, further experimental validation can confirm the effectiveness of these compounds.

REFERENCES

Adelman, Z.N., K.A. Kilcullen, R. Koganemaru, M.A. Anderson, T.D. Anderson and D.M. Miller (2011). Deep sequencing of pyrethroid-resistant bed bugs reveals multiple mechanisms of resistance within a single population. PLoS One. 6(10): e26228. https://doi.org/10.1371/journal.pone.0026228

Akhoundi, M., D. Sereno, R. Durand, A. Mirzaei, C. Bruel, P. Delaunay, P. Marty and A. Izri (2020). Bed bugs (Hemiptera, Cimicidae): overview of classification, evolution and dispersion. Int. J. Environ. Res. Public Health. 17(12): 4576. https://doi.org/10.3390/ijerph17124576

Alizadeh, I., M. Sharififard, E. Jahanifard, F. Rajaei, G. Mousavian and M. Mehraghaei (2018). Identification, knowledge and awareness of people regarding public health nuisance insect (*Cimex lectularius*) in the southwest of Iran. Jundishapur J. Health Sci. 10(3): e81133. https://doi.org/10.5812/jjhs.81133

Alshaghdali, K., M. Tasleem, R. Rezgui, T. Alharazi, T. Acar, R.F. Aljerwan, A. Altayyar, S. Siddiqui, M. Saeed, D.K. Yadav and A. Saeed (2024). *Cucumis melo* compounds: A new avenue for ALR-2 inhibition in diabetes mellitus. Heliyon. 10(15): e35255. https://doi.org/10.1016/j.heliyon.2024.e35255

Amezian, D., R. Nauen and G. Le Goff (2021). Comparative analysis of the detoxification gene inventory of four major *Spodoptera* pest species in response to xenobiotics. Insect Biochem. Mol. Biol. 138: 103646. https://doi.org/10.1016/j.ibmb.2021.103646

Bagewadi, Z.K., T.Y. Khan, B. Gangadharappa, A. Kamalapurkar, S.M. Shamsudeen and D.A. Yaraguppi (2023). Molecular dynamics and simulation analysis against superoxide dismutase (SOD) target of *Micrococcus luteus* with secondary metabolites from *Bacillus licheniformis* recognized by genome mining approach. Saudi J. Biol. Sci. 30(9): 103753. https://doi.org/10.1016/j.sjbs.2023.103753

Bhattacharya, D., J. Nowotny, R. Cao and J. Cheng (2016). 3Drefine: an interactive web server for efficient protein structure refinement. Nucleic Acids Res. 44(W1): W406-W409. https://doi.org/10.1093/nar/gkw336

Brenner, R.J. and R.D. Kramer (2019). Cockroaches (*Blattaria*). In: Medical and Veterinary Entomology, 10th Ed. GIE Media Inc.; Richmond, OH (USA). https://doi.org/10.1016/B978-0-12-814043-7.00006-6

Chan, H.H., M.F. Wajidi and J. Zairi (2014). Molecular cloning and xenobiotic induction of seven novel cytochrome P450 monooxygenases in *Aedes albopictus*. J. Insect Sci. 14(1): 163. https://doi.org/10.1093/jisesa/ieu025

Chibuye, B., I.S. Singh, L. Chimuka, M. Monyai and M.K. Kakoma (2025). Computational insights into the anti-diabetic potential of *Albizia antunesiana* (Mimosaceae) metabolites: A molecular docking, drug-likeness and ADMET analysis. Results Chem. 16: 102422. https://doi.org/10.1016/j.rechem.2025.102422

Chemical Computing Group ULC (2022). Molecular Operating Environment (MOE), version 2022.02. Chemical Computing Group ULC; Montreal, QC (Canada).

Clark, A.M., P. Labute and M. Santavy (2006). 2D structure depiction. J. Chem. Inf. Model. 46: 1107-1123. https://doi.org/10.1021/ci050550m

Cooper, R. and H. Harlan (2011). Ectoparasites, Part three: bed bugs and kissing bugs. In: The Mallis Handbook of Pest Control, 10th Ed. GIE Media Inc.; Richmond, OH (USA). pp. 587-632.

Daina, A., O. Michielin and V. Zoete (2017). SwissADME: a free web tool to evaluate pharmacokinetics, drug-likeness and medicinal chemistry friendliness of small molecules. Sci. Rep. 7: 42717. https://doi.org/10.1038/srep42717

Dang, K., S.L. Doggett, G. Veera Singham and C.Y. Lee (2017). Insecticide resistance and resistance mechanisms in bed bugs, *Cimex* spp. (Hemiptera: Cimicidae). Parasit. Vectors. 10: 318. https://doi.org/10.1186/s13071-017-2232-3

Darden, T., D. York and L. Pedersen (1993). Particle mesh Ewald: an N·log(N) method for Ewald sums in large systems. J. Chem. Physics. 98(12): 10089-10092. https://doi.org/10.1063/1.464397

Davies, T.G., L.M. Field and M.S. Williamson (2012). The re-emergence of the bed bug as a nuisance pest: implications of resistance to the pyrethroid insecticides. Med. Vet. Entomol. 26: 241-254. https://doi.org/10.1111/j.1365-2915.2011.01006.x

Dassault Systèmes BIOVIA (2021). Discovery Studio Visualizer, Version 21.1.0.20298. Dassault Systèmes; San Diego, CA (USA). https://discover.3ds.com/discovery-studio-visualizer-download

Doggett, S.L., D.E. Dwyer, P.F. Penas and R.C. Russell (2012). Bed bugs: clinical relevance and control options. Clin. Microbiol. Rev. 25(1): 164-192. https://doi.org/10.1128/cmr.05015-11

Du, Y., Y. Nomura, B.S. Zhorov and K. Dong (2016). Sodium channel mutations and pyrethroid resistance in *Aedes aegypti*. Insects. 7(4): 60. https://doi.org/10.3390/insects7040060

Feng, D., L. Ren, J. Wu, L. Guo, Z. Han, J. Yang, W. Xie, Y. Wang, F. Xu, X. Su, D. Li and H. Cao (2023). Permethrin as a potential furin inhibitor through a novel non-competitive allosteric inhibition. Molecules. 28(4): 1883. https://doi.org/10.3390/molecules28041883

Feyereisen, R. (2005). Insect cytochrome P450. Comprehensive Molecular Insect Science. 1: 1-77. https://doi.org/10.1016/b0-44-451924-6/00049-1

Gondhalekar, A.D. (2019). 2018 highlights of urban entomology. J. Med. Entomol. 56: 1188-1193. https://doi.org/10.1093/jme/tjz093

Gonzalez-Morales, M.A., Z. DeVries, A. Sierras, R.G. Santangelo, M.L. Kakumanu and C. Schal (2021). Resistance to fipronil in the common bed bug (Hemiptera: Cimicidae). J. Med. Entomol. 58(4): 1798-1807. https://doi.org/10.1093/jme/tjab040

Gore, J.C. and C. Schal (2007). Cockroach allergen biology and mitigation in the indoor environment. Annu. Rev. Entomol. 52: 439-463. https://doi.org/10.1146/annurev.ento.52.110405.091313

GROMACS Development Team (2022). GROMACS, version 2022. https://doi.org/10.5281/zenodo.7323409

Hess, B., H. Bekker, H.J. Berendsen and J.G. Fraaije (1997). LINCS: a linear constraint solver for molecular simulations. J. Comput. Chem. 18(12): 1463-1472. https://doi.org/10.1002/(SICI)1096-987X(199709)18:12<1463::AID-JCC4>3.0.CO;2-H

Hubbard, R.E. and M.K. Haider (2010). Hydrogen bonds in proteins: role and strength. In: Encyclopedia of Life Sciences. John Wiley & Sons; Chichester (UK). https://doi.org/10.1002/9780470015902.a0003011.pub2

Ibrahim, S.S., J.M. Riveron, R. Stott, H. Irving and C.S. Wondji (2016). The cytochrome P450 CYP6P4 is responsible for the high pyrethroid resistance in knockdown resistance-free *Anopheles arabiensis*. Insect Biochem. Mol. Biol. 68: 23-32. https://doi.org/10.1016/j.ibmb.2015.10.015

Ibrahim, Z.Y.U., A. Uzairu, G. Shallangwa and S. Abechi (2020). Molecular docking studies, drug-likeness and in-silico ADMET prediction of some novel beta-amino alcohol grafted 1,4,5-trisubstituted 1,2,3-triazoles derivatives as elevators of p53 protein levels. Sci. Afr. 10: e00570. https://doi.org/10.1016/j.sciaf.2020.e00570

Ibrahim, S.O., Y.O. Ayipo, H.Y. Lukman, F.A. Abubakar, A. Na'Allah, R.A. Katibi-Abdullahi and O. Atolani (2025). De novo in silico screening of natural products for antidiabetic drug discovery: ADMET profiling, molecular docking and molecular dynamics simulations. In Silico Pharmacol. 13(1): 29. https://doi.org/10.1007/s40203-025-00320-w

Irwin, J.J., K.G. Tang, J. Young, C. Dandarchuluun, B.R. Wong, M. Khurelbaatar, Y.S. Moroz, J. Mayfield, R.A. Sayle and J.J. Irwin (2020). ZINC20 - a free ultralarge-scale chemical database for ligand discovery. J. Chem. Inf. Model. 60(12): 6065-6073. https://doi.org/10.1021/acs.jcim.0c00675

Ishak, I.H., B. Kamgang, S.S. Ibrahim, J.M. Riveron, H. Irving and C.S. Wondji (2017). Pyrethroid resistance in Malaysian populations of dengue vector *Aedes aegypti* is mediated by CYP9 family of cytochrome P450 genes. PLoS Negl. Trop. Dis. 11(1): e0005302. https://doi.org/10.1371/journal.pntd.0005302

Isoherranen, N., K.L. Kunze, K.E. Allen, W.L. Nelson and K.E. Thummel (2004). Role of itraconazole metabolites in CYP3A4 inhibition. Drug Metab. Dispos. 32(11): 1121-1131. https://doi.org/10.1124/dmd.104.000315

Ko, J., H. Park, L. Heo and C. Seok (2012). GalaxyWEB server for protein structure prediction and refinement. Nucleic Acids Res. 40(W1): W294-W297. https://doi.org/10.1093/nar/gks493

Lee, J., X. Cheng, J.M. Swails, M.S. Yeom, P.K. Eastman, J.A. Lemkul, S. Wei, J. Buckner, J.C. Jeong, Y. Qi, S. Jo, V.S. Pande, D.A. Case, C.L. Brooks 3rd, A.D. MacKerell Jr., J.B. Klauda and W. Im (2016). CHARMM-GUI input generator for NAMD, GROMACS, AMBER, OpenMM and CHARMM/OpenMM simulations using the CHARMM36 additive force field. J. Chem. Theory Comput. 12(1): 405-413. https://doi.org/10.1021/acs.jctc.5b00935

Lipinski, C.A. (2000). Drug-like properties and the causes of poor solubility and poor permeability. J. Pharmacol. Toxicol. Methods. 44(1): 235-249. https://doi.org/10.1016/S1056-8719(00)00107-6

Loos, N.H.C., J.H. Beijnen and A.H. Schinkel (2023). The inhibitory and inducing effects of ritonavir on hepatic and intestinal CYP3A and other drug-handling proteins. Biomed. Pharmacother. 162: 114636. https://doi.org/10.1016/j.biopha.2023.114636

Lovell, S.C., I.W. Davis, W.B. Arendall 3rd, P.I. de Bakker, J.M. Word, M.G. Prisant, J.S. Richardson and D.C. Richardson (2003). Structure validation by C-alpha geometry: phi, psi and C-beta deviation. Proteins. 50(3): 437-450. https://doi.org/10.1002/prot.10286

Mamidala, P., A.J. Wijeratne, S. Wijeratne, K. Kornacker, B. Sudhamalla, L.J. Rivera-Vega, A. Hoelmer, T. Meulia, S.C. Jones and O. Mittapalli (2012). RNA-Seq and molecular docking reveal multi-level pesticide resistance in the bed bug. BMC Genomics. 13(1): 6. https://doi.org/10.1186/1471-2164-13-6

Miller, D.M. and J. Rogers (2012). How to identify a bed bug infestation. Virginia Cooperative Extension; Blacksburg, VA (USA). Publication No. ENTO-32NP.

Moyes, C.L., J. Vontas, A.J. Martins, L.C. Ng, S.Y. Koou, I. Dusfour, K. Raghavendra, J. Pinto, V. Corbel, J.P. David and D. Weetman (2017). Contemporary status of insecticide resistance in the major *Aedes* vectors of arboviruses infecting humans. PLoS Negl. Trop. Dis. 11(7): e0005625. https://doi.org/10.1371/journal.pntd.0005625

Myamba, J., C.A. Maxwell, A. Asidi and C.F. Curtis (2002). Pyrethroid resistance in tropical bedbugs, *Cimex hemipterus*, associated with use of treated bednets. Med. Vet. Entomol. 16(4): 448-451. https://doi.org/10.1046/j.1365-2915.2002.00389.x

Ononamadu, C.J., M. Abdalla, G.O. Ihegboro, J. Li, T.A. Owolarafe, T.D. John and Q. Tian (2021). In silico identification and study of potential anti-mosquito juvenile hormone binding protein (MJHBP) compounds as candidates for dengue virus-vector insecticides. Biochem. Biophys. Rep. 28: 101178. https://doi.org/10.1016/j.bbrep.2021.101178

Parrinello, M. and A. Rahman (1981). Polymorphic transitions in single crystals: A new molecular dynamics method. J. Appl. Phys. 52(12): 7182-7190. https://doi.org/10.1063/1.328693

Ramirez, D. and J. Caballero (2018). Is it reliable to take the molecular docking top scoring position as the best solution without considering available structural data? Molecules. 23(5): 1038. https://doi.org/10.3390/molecules23051038

Rana, N., P. Solanki, R. Mehra and A. Manhas (2025). Identification of natural compound inhibitors for substrate-binding site of MTHFD2 enzyme: Insights from structure-based drug design and biomolecular simulations. Chem. Phys. Impact. 10: 100809. https://doi.org/10.1016/j.chphi.2024.100809

Romero, A., M.F. Potter, D.A. Potter and K.F. Haynes (2007). Insecticide resistance in the bed bug: a factor in the pest's sudden resurgence? J. Med. Entomol. 44(2): 175-178. https://doi.org/10.1093/jmedent/44.2.175

Romero, A. and T.D. Anderson (2016). High levels of resistance in the common bed bug, *Cimex lectularius* (Hemiptera: Cimicidae), to neonicotinoid insecticides. J. Med. Entomol. 53(3): 727-731. https://doi.org/10.1093/jme/tjv253

Rosado-Solano, D.N., M.A. Barón-Rodríguez, P.L. Sanabria Florez, L.K. Luna-Parada, C.E. Puerto-Galvis, A.F. Zorro-González, V.V. Kouznetsov and L.Y. Vargas-Méndez (2019). Synthesis, biological evaluation and in silico computational studies of 7-chloro-4-(1H-1,2,3-triazol-1-yl)quinoline derivatives: search for new controlling agents against *Spodoptera frugiperda* (Lepidoptera: Noctuidae) larvae. J. Agric. Food Chem. 67: 9210-9219. https://doi.org/10.1021/acs.jafc.9b01067

Saini, V. and A. Kumar (2014). Computer aided pesticide design: A rational tool for supplementing DDT lacunae. Chem. Sci. Trans. 3(9): 676-688. https://doi.org/10.7598/cst2014.719

Saleh, M.A., M.A. El-Badry and R.E.E. El-Rashedy (2021). Novel 6-hydroxyquinolinone derivatives: Design, synthesis, antimicrobial evaluation, in silico study and toxicity profiling. J. Comput. Chem. 42(22): 1561-1578. https://doi.org/10.1002/jcc.26693

Senthil, R., S. Usha and K.M. Saravanan (2019). Importance of fluctuating amino acid residues in folding and binding of proteins. Avicenna J. Med. Biotechnol. 11(4): 339-343. PMID: 31908743.

Smith, L.B., C. Sears, H. Sun, R.W. Mertz, S. Kasai and J.G. Scott (2019). CYP-mediated resistance and cross-resistance to pyrethroids and organophosphates in *Aedes aegypti* in the presence and absence of kdr. Pestic. Biochem. Physiol. 160: 119-126. https://doi.org/10.1016/j.pestbp.2019.07.011

Soh, L.S. and G. Veera Singham (2021). Cuticle thickening associated with fenitrothion and imidacloprid resistance and influence of voltage-gated sodium channel mutations on pyrethroid resistance in the tropical bed bug, *Cimex hemipterus*. Pest Manag. Sci. 77(11): 5202-5212. https://doi.org/10.1002/ps.6561

Souza, F.F., J.F. Vilachã, O.S. Campos and H. de Paula (2025). Prediction of novel insecticides for malaria prevention: virtual screening and molecular dynamics of AgAChE inhibitors. Drugs Drug Candidates. 4(3): 41. https://doi.org/10.3390/ddc4030041

Strode, C., C.S. Wondji, J.P. David, N.J. Hawkes, N. Lumjuan, D.R. Nelson, D.R. Drane, S.H. Karunaratne, J. Hemingway, W.C. Black 4th and H. Ranson (2008). Genomic analysis of detoxification genes in the mosquito *Aedes aegypti*. Insect Biochem. Mol. Biol. 38(1): 113-123. https://doi.org/10.1016/j.ibmb.2007.09.007

Sutton, D., A.M. Butler, L. Nadin and M. Murray (1997). Role of CYP3A4 in human hepatic diltiazem N-demethylation: inhibition of CYP3A4 activity by oxidized diltiazem metabolites. J. Pharmacol. Exp. Ther. 282(1): 294-300. https://doi.org/10.1016/S0022-3565(24)36788-6

Tian, W., C. Chen, X. Lei, J. Zhao and J. Liang (2018). CASTp 3.0: computed atlas of surface topography of proteins. Nucleic Acids Res. 46(W1): W363-W367. https://doi.org/10.1093/nar/gky473

Tice, C.M. (2001). Selecting the right compounds for screening: Does Lipinski's rule of 5 for pharmaceuticals apply to agrochemicals? Pest Manag. Sci. 57(1): 3-16. https://doi.org/10.1002/1526-4998(200101)57:1<3::AID-PS269>3.0.CO;2-6

Turner, P.J. (2009). Xmgr/Grace plotting software documentation. ACE/gr Development Team. Available at: https://plasma-gate.weizmann.ac.il/Xmgr/doc/ (accessed August 2026).

UniProt Consortium (2025). UniProt: the universal protein knowledgebase in 2025. Nucleic Acids Res. 53(D1): D609-D617. https://doi.org/10.1093/nar/gkae1010

Veber, D.F., S.R. Johnson, H.Y. Cheng, B.R. Smith, K.W. Ward and K.D. Kopple (2002). Molecular properties that influence the oral bioavailability of drug candidates. J. Med. Chem. 45(12): 2615-2623. https://doi.org/10.1021/jm020017n

Wass, M.N., L.A. Kelley and M.J. Sternberg (2010). 3DLigandSite: predicting ligand-binding sites using similar structures. Nucleic Acids Res. 38(Suppl. 2): W469-W473. https://doi.org/10.1093/nar/gkq406

Waterhouse, A., M. Bertoni, S. Bienert, G. Studer, G. Tauriello, R. Gumienny, F.T. Heer, T.A.P. de Beer, C. Rempfer, L. Bordoli, R. Lepore and T. Schwede (2018). SWISS-MODEL: homology modelling of protein structures and complexes. Nucleic Acids Res. 46(W1): W296-W303. https://doi.org/10.1093/nar/gky427

Wiederstein, M. and M.J. Sippl (2007). ProSA-web: interactive web service for the recognition of errors in three-dimensional structures of proteins. Nucleic Acids Res. 35(W2): W407-W410. https://doi.org/10.1093/nar/gkm290

Wismer, T. (2016). Feline toxins: recognition, diagnosis, treatment. In: August's Consultations in Feline Internal Medicine, Volume 7. Elsevier; St. Louis, MO (USA). pp. 791-798. https://doi.org/10.1016/B978-0-323-22652-3.00079-7

World Health Organization (2020). Vector-borne diseases. Fact Sheet. World Health Organization; Geneva (Switzerland). https://www.who.int/news-room/fact-sheets/detail/vector-borne-diseases

Xiong, G., Z. Wu, J. Yi, L. Fu, Z. Yang, C. Hsieh, M. Yin, X. Zeng, C. Wu, A. Lu, X. Chen, T. Hou and D. Cao (2021). ADMETlab 2.0: an integrated online platform for accurate and comprehensive predictions of ADMET properties. Nucleic Acids Res. 49(W1): W5-W14. https://doi.org/10.1093/nar/gkab255

Yang, J., A. Roy and Y. Zhang (2013). Protein-ligand binding site recognition using complementary binding-specific substructure comparison and sequence profile alignment. Bioinformatics. 29(20): 2588-2595. https://doi.org/10.1093/bioinformatics/btt447

Zhang, Y. and J. Skolnick (2004). Automated structure prediction of weakly homologous proteins on a genomic scale. Proc. Natl. Acad. Sci. U.S.A. 101(20): 7594-7599. https://doi.org/10.1073/pnas.0305695101

Zhao, X.J., E. Koyama and T. Ishizaki (1999). An in vitro study on the metabolism and possible drug interactions of rokitamycin, a macrolide antibiotic, using human liver microsomes. Drug Metab. Dispos. 27(7): 776-785. https://doi.org/10.1016/S0090-9556(24)15225-7

Zhou, X., K. Qian, Y. Tong, J.J. Zhu, X. Qiu and X. Zeng (2014). De novo transcriptome of the Hemimetabolous German cockroach (*Blattella germanica*). PLoS One. 9(9): e106932. https://doi.org/10.1371/journal.pone.0106932

Zhou, X., W. Zheng, Y. Li, R. Pearce, C. Zhang, E.W. Bell, G. Zhang and Y. Zhang (2022). I-TASSER-MTD: a deep-learning-based platform for multi-domain protein structure and function prediction. Nat. Protoc. 17(10): 2326-2353. https://doi.org/10.1038/s41596-022-00728-0

Zhu, F., H. Gujar, J.R. Gordon, K.F. Haynes, M.F. Potter and S.R. Palli (2013). Bed bugs evolved unique adaptive strategy to resist pyrethroid insecticides. Sci. Rep. 3: 1456. https://doi.org/10.1038/srep01456